



# Measurement of the data to simulation ratio of photon detection efficiency of the Belle II electromagnetic calorimeter using radiative muon pair events

Henrikas Svidras, Arthur Bolz, Ilya Komarov, Markus Röhrken, Simon Wehle,  
Kerstin Tackmann

DESY  
Hamburg, Germany

August 16, 2021

## Abstract

This note presents photon detection efficiency data-to-simulation ratio distributions in the barrel region of the electromagnetic calorimeter of the Belle II detector at the SuperKEKB asymmetric energy electron-positron collider. They are computed using  $71.2 \text{ fb}^{-1}$  of experimental data collected by the Belle II detector and the official Belle II Monte Carlo simulation. An initial-state high energy photon from  $e^+e^- \rightarrow \mu^+\mu^-(\gamma_{\text{ISR}})$  is searched by predicting its momentum from missing momentum of the dimuon system. The data-to-simulation ratios of the detection efficiency are presented as functions of missing momentum and its angular directions.

## I. INTRODUCTION

Belle II is a  $B$ -factory experiment at the SuperKEKB electron-positron collider in Tsukuba, Japan. Many analyses performed on the data collected at Belle II rely on high-energy photons in the final-state, such as  $B \rightarrow X_{s,d}\gamma$ . Therefore, a good simulation of photon detection efficiency of the electromagnetic calorimeter (ECL) of Belle II is crucial. The study presented here measures the data-to-simulation photon detection efficiency ratios, using high-energy photons emitted in the initial state of  $e^+e^- \rightarrow \mu^+\mu^-$  transitions. The study is performed for photons in the barrel region (polar angle between  $50 - 110^\circ$ .)

The study uses experimental data collected by the Belle II detector at the  $\Upsilon(4S)$  mass ( $63 \text{ fb}^{-1}$ ) and 60 MeV below ( $7 \text{ fb}^{-1}$ ). Simulated events from official Belle II Monte Carlo (MC) campaigns are used. For signal events, the study uses a simulated sample of  $60 \text{ fb}^{-1}$   $e^+e^- \rightarrow \mu^+\mu^-(\gamma_{\text{ISR}})$  events. Additional  $100 \text{ fb}^{-1}$  of simulated samples are used to describe dominant background processes  $e^+e^- \rightarrow u\bar{u}, d\bar{d}, c\bar{c}, s\bar{s}, B\bar{B}, \tau^+\tau^-$ .

The measurement selects  $e^+e^- \rightarrow \mu^+\mu^-(\gamma_{\text{ISR}})$  events, where  $\gamma_{\text{ISR}}$  is a photon radiated from the initial  $e^+e^-$  state, as described in Section II. The schematic representation of the measurement is depicted in Figure 1. Using constraints from the well-defined initial  $e^+e^-$  state, the photon energy and direction are predicted from the missing momentum of the dimuon system. From here on, the missing momentum will be referred to as the ‘‘recoil’’, its magnitude denoted as  $p_{\text{Recoil}}$ , and its direction as  $\theta_{\text{Recoil}}$  and  $\phi_{\text{Recoil}}$ , representing the polar and the azimuthal angle, respectively. The invariant mass associated with the recoil is denoted as  $m_{\text{Recoil}}$ .

A corresponding photon cluster is searched in a cone around the direction of the recoil. This will be referred to as ‘‘matching’’ and is explained in depth in Section III. The matching efficiency is then given as:

$$\varepsilon_{\text{matching}}(p_{\text{Recoil}}, \theta_{\text{Recoil}}, \phi_{\text{Recoil}}) = \frac{N_{\text{matched}}}{N_{\text{selected}}}. \quad (1)$$

Here, the  $N_{\text{selected}}$  corresponds to the number of events passing the event selection before matching. Conversely,  $N_{\text{matched}}$  is the number of events where the  $p_{\text{Recoil}}$  correctly pointed to a reconstructed  $\gamma$  cluster. To minimise the extent of systematic effects related to the measurement method, the study provides data-to-simulation ratios,  $\frac{\varepsilon_{\text{DATA}}}{\varepsilon_{\text{MC}}}$ , rather than absolute efficiencies. The associated uncertainties and efficiency ratios are presented in Sections IV and V.

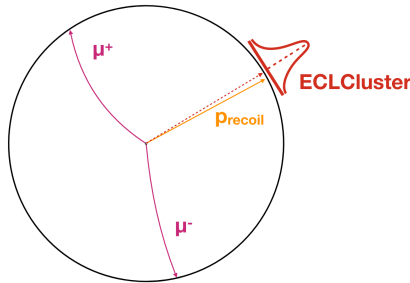


FIG. 1: The schematic representation of events used in the study. The momentum of the  $\gamma_{\text{ISR}}$  is predicted using the missing momentum of the dimuon system. A corresponding ECL cluster is then searched.

## II. SELECTION OF RECOIL SYSTEM AND PHOTON CANDIDATES

Events are only considered if there are exactly two tracks that 1) leave energy deposits in the calorimeter that are not larger than 300 MeV and less than 80% of their total momentum, 2) are coming from the interaction point, and 3) have a momentum of at least 1 GeV/c. To reduce the impact of background processes faking missing momentum, such as  $e^+e^- \rightarrow \tau^+\tau^-$  (neutrinos in the final state), a  $m_{\text{Recoil}}^2 < 2 \text{ GeV}^2/c^4$  is required. This heavily suppresses most of the background processes. Furthermore, clear  $\mu$  and recoil angular separation by at least 0.3 rad in polar and azimuthal angle is required. After these selections, events where  $p_{\text{Recoil}} > 0.2 \text{ GeV}/c$  are considered to have passed the event selection. The experimental data agrees with simulation well as shown in Figure 2(a). For further calculations, the leftover events estimated from simulated background processes are subtracted from the selected distributions.

To suppress photons originating from beam background, photon candidate-based requirements are defined. The ECL cluster timing is required to be within  $\pm 200$  ns and have a minimum energy in the center-of-mass frame of 75 MeV.

## III. RECOIL SYSTEM TO PHOTON MATCHING PROCEDURE

Events with recoil that match the criteria described in the previous sections are then used in the matching procedure. Photon candidates that are within a 0.3 rad spatial cone of the recoil direction and satisfy  $1.2 > E_\gamma/p_{\text{Recoil}} > 0.5$  requirement are considered as matched. In case the recoil can be matched to multiple photons satisfying these requirements, such matches are considered invalid. However, cases where this procedure matches to multiple photons are rare and at sub percent level. After the matching step, experimental data agrees with the simulated samples well and is shown in Figure 2(b). For further calculations, the leftover events estimated from simulated background processes are subtracted from the matched distributions.

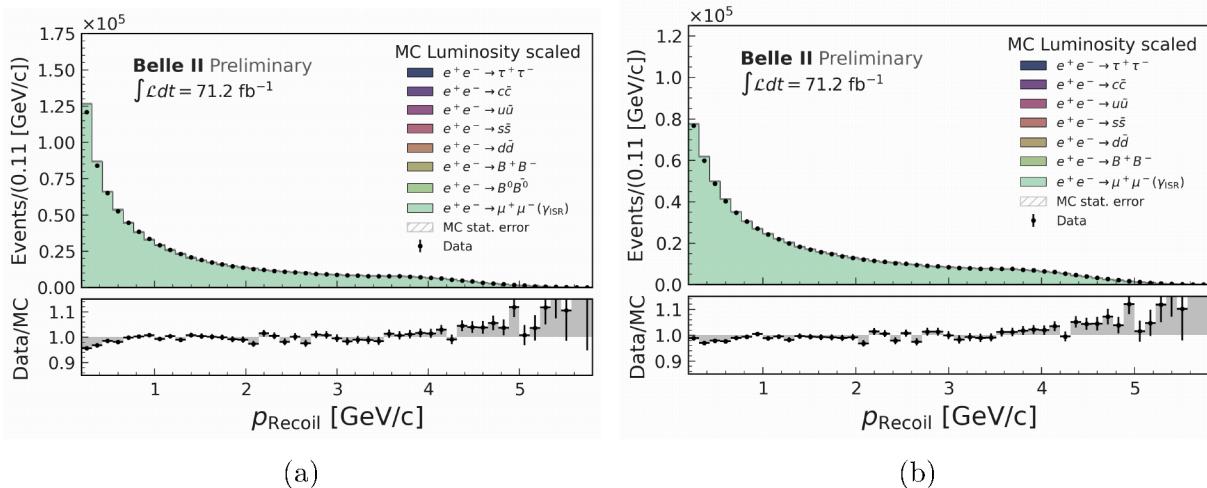


FIG. 2: Number of events in data and simulation from stacked signal and background processes compared after the a) recoil selection and b) matching selection. The simulated event yields are normalised to the luminosity of the data sample. Only statistical uncertainties are shown here.

## IV. UNCERTAINTY ESTIMATION

Systematic uncertainties are derived from the difference between the ratios calculated with nominal selections and the ratios calculated by tightening and loosening the selections and matching requirements. Furthermore, the difference in central value between the ratio with simulated background subtraction performed and not performed is assigned as a systematic uncertainty related to the background modelling. Lastly, the shift in central value induced by a tight cut on the photon isolation from the muon ( $> 1$  rad in 3D angle) is added as a systematic uncertainty. The full list of uncertainties is given in Table I. Overall, the systematic uncertainties are smaller than 1% and statistical uncertainties smaller than 0.1%. The largest contributions to systematic uncertainties arise from the isolation requirement,  $m_{\text{Recoil}}^2$  variation and variation of the upper limit of energy deposit associated to muon tracks. The first two relate to background process suppression and modelling, whereas the latter is related to muon track quality.

TABLE I: This table summarises variations in selection and matching used for systematic error estimation. The shown systematic uncertainty is for the entire  $p_{\text{Recoil}} > 0.2$  GeV/c range.

Event selection-related	Varied value	Systematic uncertainty on $\frac{\varepsilon_{\text{DATA}}}{\varepsilon_{\text{MC}}}$
Variation of the upper limit of energy associated to muon tracks	$300^{+50}_{-50}$ MeV	$+0.0014$ $-0.0000$
Removal of $E_{\mu,\text{cluster}}$ upper limit	$> 0$ MeV	negligible
Variation of the squared mass of recoiling system	$< 2^{+1}_{-1}$ GeV $^2/c^4$	$+0.0015$ $-0.0003$
Varying the separation between $\mu$ and recoiling system in polar/azimuthal angle	$> 0.3^{+0.1}_{-0.1}$ rad	negligible
Matching-related	Varied value	
Matching window for the photon energy to recoil system momentum	$0.5^{+0.1}_{-0.1} - 1.2^{+0.1}_{-0.1}$	$+0.0007$ $-0.0020$
Matching cone size in polar/azimuthal around the recoil system	$< 0.3^{+0.1}_{-0.1}$ rad	negligible
Background modelling related	Varied value	
Tight muon/recoil isolation cut in 3D angle	$> 1$ rad	$+0.0000$ $-0.0083$
Subtraction of leftover background	Monte Carlo subtraction	$+0.0000$ $-0.0002$

## V. DATA-TO-SIMULATION EFFICIENCY RATIOS

The matching efficiency as defined in Equation (1) is computed from the number of selected and matched events, corrected for backgrounds, as a function of the magnitude and direction of the missing momentum. The result as a function of  $p_{\text{Recoil}}$  is shown in Figure 3.

One can note the apparent decrease in matching efficiency with decreasing  $p_{\text{Recoil}}$ . This effect is attributed to the limitation of the measurement method, where multiple  $\gamma_{\text{ISR}}$  in the event cause the missing momentum of the dimuon system to fail to predict the direction of the photon. At low  $p_{\text{Recoil}}$ , the effect of the secondary ISR photon is larger leading to a more frequent mismatch. This effect, however, is described in simulation and can be suppressed in a ratio, as apparent from the  $\frac{\varepsilon_{\text{DATA}}}{\varepsilon_{\text{MC}}}$  distribution which is consistent with 1 in the entire  $p_{\text{Recoil}} > 0.2$  GeV/c range. Studies in Monte Carlo simulation show that performing the study exclusively on events with up to one ISR photon as a generator level requirement brings the  $\varepsilon$  in simulation to  $> 99\%$  for  $p_{\text{Recoil}} > 0.5$  GeV/c.

For  $\theta_{\text{Recoil}}$  (Figure 4) and  $\phi_{\text{Recoil}}$  (Figure 5), the matching efficiency is flat for the entire barrel region, except for  $\theta_{\text{Recoil}} \approx \pi/2$  where additional material is present due to ECL supporting structures in the Belle II detector.

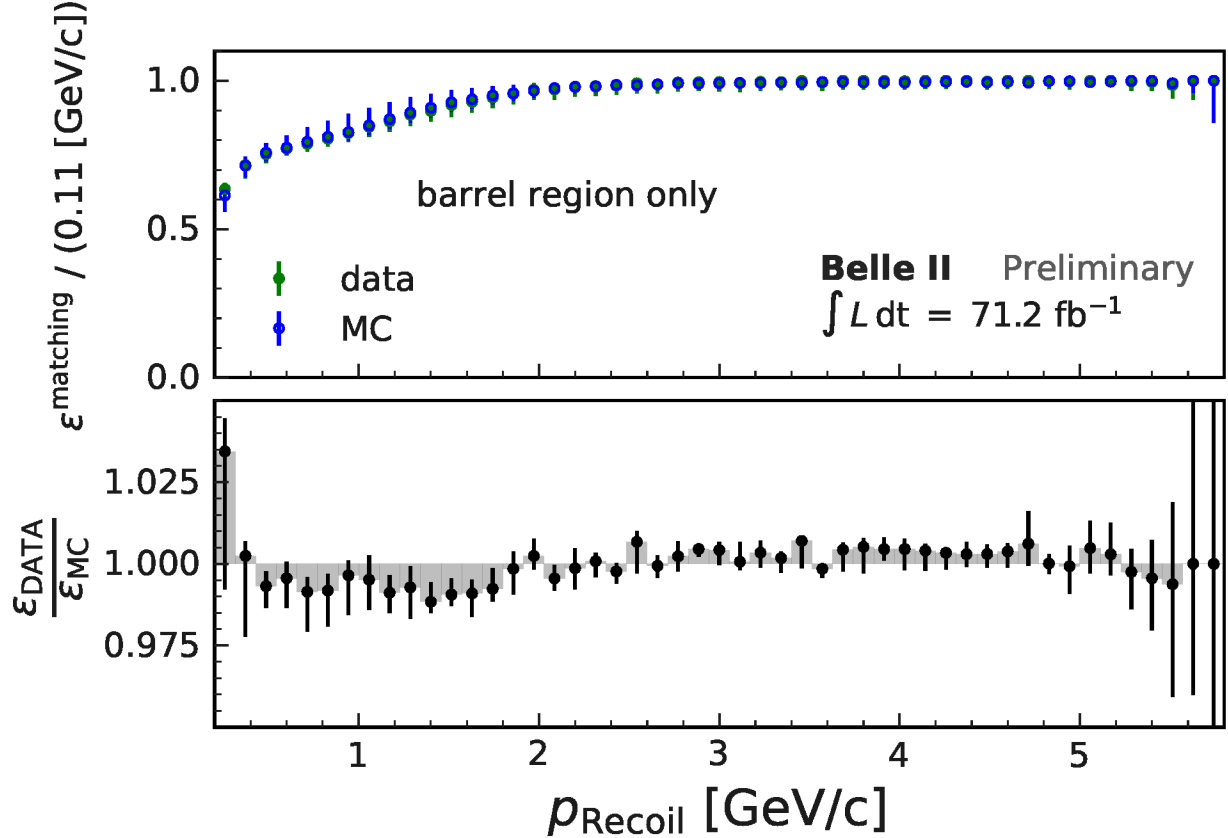


FIG. 3: The upper subplot shows the efficiency to match  $p_{\text{Recoil}}$  to a photon ( $\epsilon^{\text{matching}}$ ) as a function of  $p_{\text{Recoil}}$  region in data and simulation. The lower subplot shows the ratio of the two matching efficiencies. The decrease in absolute matching efficiencies towards lower  $p_{\text{Recoil}}$  values is due to the limitation of the measurement method used, as multiple  $\gamma_{\text{ISR}}$  emission causes  $p_{\text{Recoil}}$  to fail to predict the  $\gamma$  momentum. The data-simulation ratio is in agreement with 1.0 in the entire range.

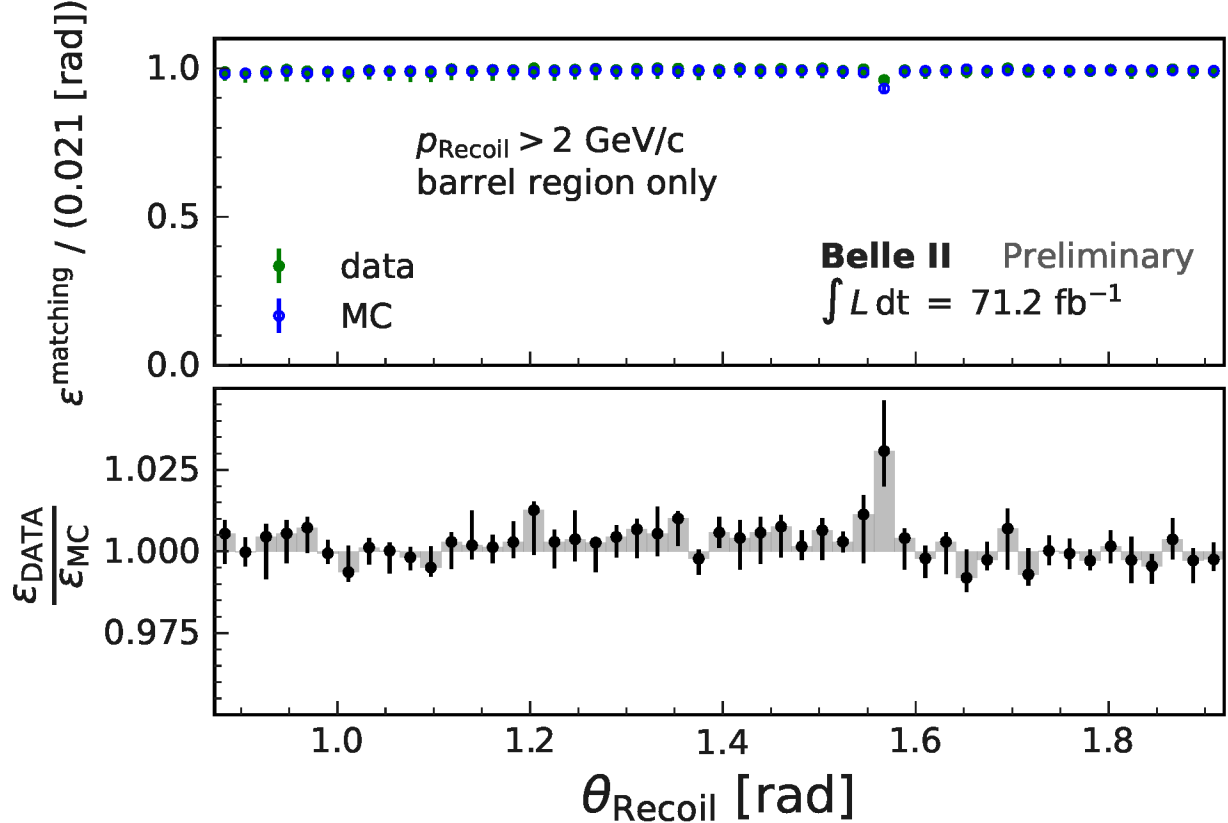


FIG. 4: The upper subplot shows the efficiency to match  $p_{\text{Recoil}}$  to a photon ( $\varepsilon^{\text{matching}}$ ) as a function of  $\theta_{\text{Recoil}}$  region in data and simulation. The ratios and efficiencies depicted are computed for events with  $p_{\text{Recoil}} > 2 \text{ GeV}/c$ . The data-simulation ratio is in agreement with 1.0 in most of the barrel region. The deviation around  $\theta \approx \pi/2$  is related to additional material of supporting structures in the electromagnetic calorimeter, which suggests that material modelling in the region could be improved..

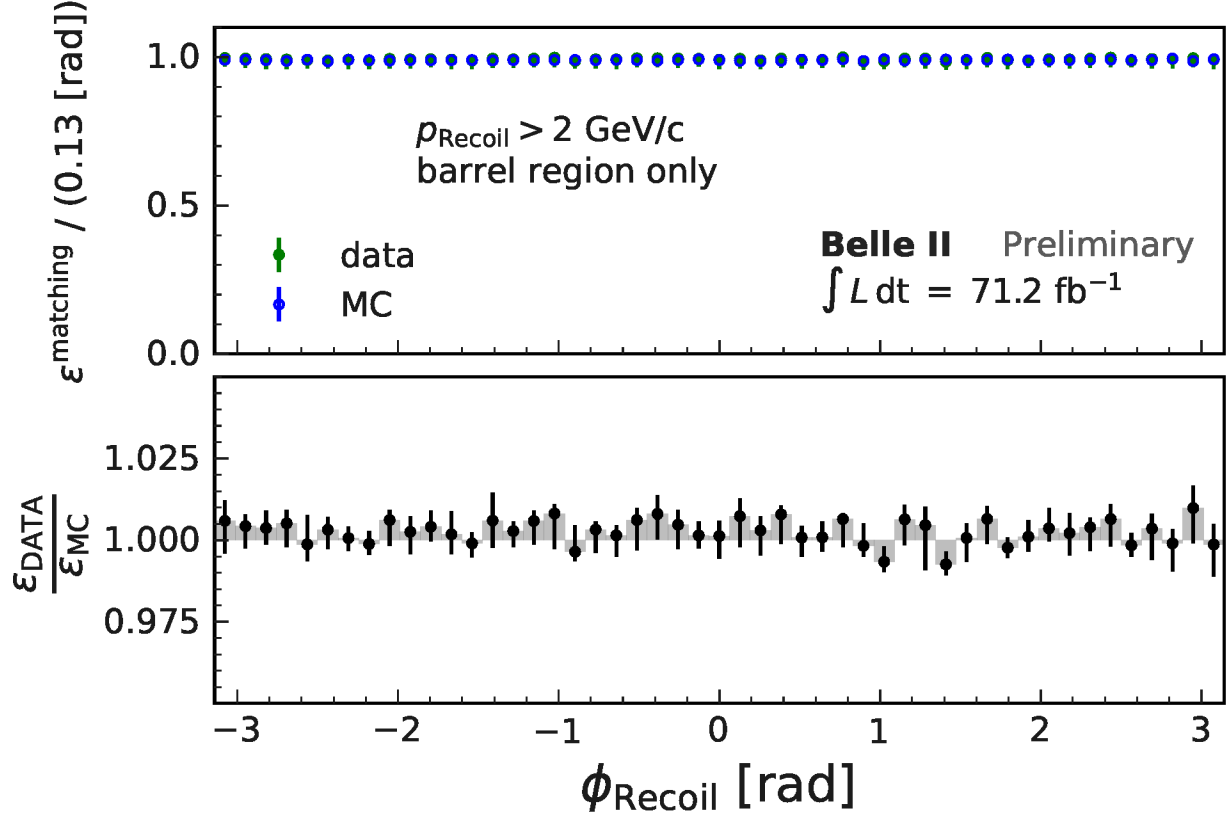


FIG. 5: The upper subplot shows the efficiency to match  $p_{\text{Recoil}}$  to a photon ( $\epsilon^{\text{matching}}$ ) as a function of  $\phi_{\text{Recoil}}$  region in data and simulation. The lower subplot shows the ratio of the two matching efficiencies. The ratios and efficiencies depicted are computed for events with  $p_{\text{Recoil}} > 2 \text{ GeV}/c$ . The data-simulation ratio is in agreement with 1.0.